Development 130, 439-449

doi:10.1242/dev.00242

Functional subdivision of trunk visceral mesoderm parasegments in *Drosophila* is required for gut and trachea development

Chie Hosono, Katsumi Takaira, Ryo Matsuda and Kaoru Saigo*

Department of Biophysics and Biochemistry, Graduate School of Science, University of Tokyo, 7-3-1 Hongo, Bunkyo-ku, Tokyo 113-0033, Japan

*Author for correspondence (e-mail: saigo@biochem.s.u-tokyo.ac.jp)

Accepted 31 October 2002

SUMMARY

In *Drosophila*, trunk visceral mesoderm, a derivative of dorsal mesoderm, gives rise to circular visceral muscles. It has been demonstrated that the trunk visceral mesoderm parasegment is subdivided into at least two domains by *connectin* expression, which is regulated by Hedgehog and Wingless emanating from the ectoderm. We now extend these findings by examining a greater number of visceral mesodermal genes, including *hedgehog* and *branchless*. Each visceral mesodermal parasegment appears to be divided into five or six regions, based on differences in expression patterns of these genes. Ectodermal Hedgehog and Wingless differentially regulate the expression of these metameric targets in trunk visceral mesoderm. *hedgehog* expression in trunk visceral mesoderm is responsible for maintaining its own expression and *con* expression. *hedgehog* expressed in visceral mesoderm parasegment 3 may also be required for normal *decapentaplegic* expression in this region and normal gastric caecum development. *branchless* expressed in each trunk visceral mesodermal parasegment serves as a guide for the initial budding of tracheal visceral branches. The metameric pattern of trunk visceral mesoderm, organized in response to ectodermal instructive signals, is thus maintained at a later time via autoregulation, is required for midgut morphogenesis and exerts feedback effect on trachea, ectodermal derivatives.

Key words: *Drosophila melanogaster*, Visceral mesoderm, Visceral mesoderm parasegment, *hedgehog*, *wingless*, *branchless*, *tinman*, *decapentaplegic*, Trachea, Gastric caecum

INTRODUCTION

Interactions between germ layers are essential for the formation and development of tissues and organs in embryogenesis. *Drosophila* visceral mesoderm would appear to be a good system for molecular and genetic study of these processes. Midgut visceral mesoderm consists of trunk and caudal visceral mesoderm, which, respectively, give rise to circular and longitudinal muscles (Campos-Ortega and Hartenstein, 1997). The formation and specification of trunk visceral mesoderm (VM), require overlaying ectodermal signals (Azpiazu et al., 1996; Riechmann et al., 1997), while it regulates the development of underlying endodermal tissue (Bienz, 1994). Gut digestion is carried out under the control of visceral muscles (Dettman et al., 1996).

During gastrulation and subsequent stages, future mesoderm invaginates, spreading laterally and dorsally to form a rather uniform cell monolayer (mesoderm), in close contact with overlaying ectoderm (Leptin and Grunewald, 1990). As with ectoderm, the mesoderm consists of parasegmental units (PSs), each divided into *even-skipped* (*eve*) and *sloppy-paired* (*slp*) domains along the anteroposterior (AP) axis (Borkowski et al., 1995; Azpiazu et al., 1996; Riechmann et al., 1997). The concerted action of Decapentaplegic (DPP), which emanates from the dorsal ectoderm, and Wingless (WG) and Hedgehog (HH), both of which are secreted from alternating ectodermal sources along the AP axis, must be available for further subdivision of mesodermal PS and subsequent mesodermal cell differentiation (reviewed by Baylies, 1998).

VM development begins with VM competent cell specification within the dorsoanterior quarter of each mesodermal parasegment. VM competent regions may be defined using expression of *bagpipe* (*bap*), a homeobox gene, which is positively regulated by *hh*, *dpp* and *tinman* (*tin*), and negatively by *wg* (Staehling-Hampton et al., 1994; Frasch, 1995, Azpiazu et al., 1996; Lee and Frasch, 2000). During stage 10, the anterior terminus of each VM competent region always appears to touch an anteroposterior compartment border (AP border) or ectodermal WG source; the putative posterior terminus, which is initially situated halfway between two flanking AP borders, approaches the neighboring ectodermal WG source at late stage 10 (Borkowski et al., 1995; Azpiazu et al., 1996; Weiss et al., 2001). Each VM competent region splits into two regions that consist of peripheral columnar cells, which may constitute a VM progenitor region destined for founder myoblasts of circular muscles, and another comprising hexagonal cells, future fusion-competent visceral myoblasts (San Martin et al., 2001; Klapper et al., 2002). A string-like VM arch structure, positive for Fasciclin 3 (FAS3), is formed through head-to-tail connection of

neighboring VM progenitor regions. VM progenitor cells eventually fuse with fusion-competent myoblasts to form circular visceral muscles (San Martin et al., 2001; Klapper et al., 2002).

As with mesoderm, VM possesses segmental modules (trunk visceral mesodermal parasegments; VM-PSs). Connectin (CON), a cell adhesion molecule, is expressed in VM and its expression is well aligned with ectodermal parasegment borders (Bilder and Scott, 1998). Bilder and Scott (Bilder and Scott, 1998) considered VM-PSs to consist of CON-positive and -negative regions, and suggested that *con* expression in VM-PSs is positively and negatively regulated by ectodermal *hh* and *wg*, respectively.

VM confers positional cues to the endoderm (Szuts et al., 1998). *dpp* and *wg* are expressed in VM-PS7 and VM-PS8, respectively. They are regulated by a positive feedback loop and, together, control *labial* expression in underlying endoderm (Hoppler and Bienz, 1995; Bienz, 1997).

Attention in this study is directed to cell fate diversification within each VM-PS. We first show that VM-PSs are subdivided into five or six regions based on differences in the expression of five VM-PS genes, which include *hh* and *branchless* (*bnl*) (Sutherland et al., 1996). Shift-up/down experiments indicate that VM-PS gene expression is regulated by ectodermal HH and WG signals in different ways. Finally, we show that *hh* expression in VM-PS3 is required for normal gastric caecum development, while metameric expression of *bnl* in VM serves as a guidance of the initial budding of visceral branches (VB) of the trachea, an ectodermal organ.

MATERIALS AND METHODS

Fly stocks

Canton S was used as wild type. Mutant strains, enhancer-trap lines and GAL4-UAS lines used are: hh^{13C}, wg^{CX4}, hh^{9K}, wg^{IL4}, VM-*hh-lacZ* (K. T., unpublished), *bap-lacZ* (baplac4.5#23) (Azpiazu and Frasch, 1993), *ftz-lacZ* (Hiromi et al., 1985), UAS-*hh* (Suzuki and Saigo, 2000), UAS-*wg*, UAS-*ciNZn* (Hepker et al., 1997), UAS-*dTCF*-ΔN (Cavallo et al., 1998), *twi*-GAL4, 24B-GAL4, *bap*-GAL4 (Zaffran et al., 2001) and 48Y-GAL4. See FlyBase for fly strains whose sources are not indicated. Genotypes of embryos were identified by the aid of *lacZ* or GFP balancers. Embryonic stages were determined according to Campos-Ortega and Hartenstein (Campos-Ortega and Hartenstein, 1985). All the experiments other than temperature-shift-experiments were carried out at 25°C.

Histochemistry

Immunohistochemistry was carried out as described previously (Suzuki and Saigo, 2000). Primary antibodies used are rabbit anti-HH (1:1000) (Tabata and Kornberg, 1994), mouse anti-WG (mab4D4, DSHB), rabbit anti-TIN (1:900; generously provided by Manfred Frasch), mouse anti-CON (1:5) (Meadows et al., 1994), mouse anti-PTC (1:200) (Capdevila et al., 1994), mouse anti-FAS3 (mab7G10, DSHB), mouse anti-FAS2 (1:10) (Grenningloh et al., 1991) and anti-*lacZ* protein [rabbit polyclonal (Cappel); mouse monoclonal (Promega)] antibodies. TSA indirect amplification kit (Renaissance) was used if necessary. Double fluorescence labeling with riboprobe and antibody was carried out as described by Suzuki et al. (Suzuki and Saigo, 2000). cDNA clones used as hybridization probes were *bnl* (Sutherland et al., 1996), *bap* (Azpiazu and Frasch, 1993), *Wnt4* (Graba et al., 1995), *hh* (Tashiro et al., 1993), *dpp* (Sato and Saigo, 2000) and *vein* (Yarnitzky et al., 1997).

Temperature shift experiments

Temperature shift-up/down experiments were carried out essentially as described (Matsuzaki and Saigo, 1996). hh^{9K}/hh^{13C} and wg^{IL114} flies were used as hh^{ts} and wg^{ts} mutants, respectively. Developmental times for shift-up/down experiments are normalized to growth rate at 25°C and shown by hours after egg laying (AEL).

Gut phenotype analysis

Larvae with appropriate genotypes were identified by the aid of the GFP-balancer and dissected guts were stained with phalloidin-FITC (Molecular Probes) as described previously (Hoppler and Bienz, 1994).

RESULTS

Metameric expression of *hh* in VM and subdivision of VM-PSs into several regions

Enhancer analysis of *hh* demonstrated that one *hh* enhancer fragment (Sph-*hh*) is capable of inducing reporter gene expression segmentally in VM (K. T. and K. S., unpublished) (Fig. 1A2). *lacZ* driven by Sph-*hh* and also *hh* RNA and protein were expressed as ten VM patches, well aligned with overlaying ectodermal *hh* stripes (Fig. 1A1,B). Expression of *hh* RNA in late stage 11 embryos almost entirely overlapped with that of *lacZ* driven by Sph-*hh* (Fig. 1A1-A3). Consequently, *hh* was concluded to be expressed in VM in a metameric fashion. *hh* expressed in VM is hereafter referred to as VM-*hh*. VM-*hh* RNA expression, which is initially detected at mid-stage 11, diminished at stage 12, but was weakly detectable until stage 15. Sph-*hh*-driven *lacZ* (VM-*hh-lacZ*) signals were detected up to stage 16. *ptc*, a general target gene of HH signaling (reviewed by Alcedo and Noll, 1997), was expressed in or around *hh*-expressing VM cells at mid stage 12 (Fig. 1C), suggesting autocrine and paracrine functions of VM-HH. Even-numbered VM-PSs in early mesoderm is marked by *ftz-lacZ* expression (Fig. 1D2) (Tremml and Bienz, 1989). *hh* RNA staining of late stage 11 *ftz-lacZ* embryos disclosed VM-*hh* expression in the anterior terminal region of each VM-PS (Fig. 1D); VM-*hh* expression was absent from VM-PS2.

Besides *hh* and *ptc*, four other genes appear to belong to the VM metameric gene family (Fig. 2A-D). Metameric CON expression occurs in VM between mid-stage 11 and stage 15 (Bilder and Scott, 1998). Staining for CON and VM-*hh-lacZ* (Fig. 2E) demonstrated that CON is expressed in cells situated on the anterior side of each VM-PS. The *con* expression domain was broader than that of *hh*. *con* expression was somewhat weak near the VM-PS border.

Metameric RNA expression of *bnl*, which encodes a ligand for Breathless FGF receptor (Sutherland et al., 1996), was first observed as 12 patches at mid stage 11 (Fig. 2A). *bnl* RNA expression became homogeneous and then diminished during stage 12 (data not shown). *tin* is a homeobox gene that is required for dorsal mesodermal development (Azpiazu and Frasch, 1993; Bodmer, 1993). At early stage 10, *tin* is expressed throughout the dorsal mesoderm from which VM is derived. Metameric TIN expression became evident by early stage 11 (Azpiazu and Frasch, 1993) (Fig. 2B, Fig. 3L). TIN expression decreased during stage 12. Expression of *bap*, another homeobox gene required for VM development, can be monitored by *bap 4.5#23* (*bap-lacZ*) (Fig. 2C). Staining for

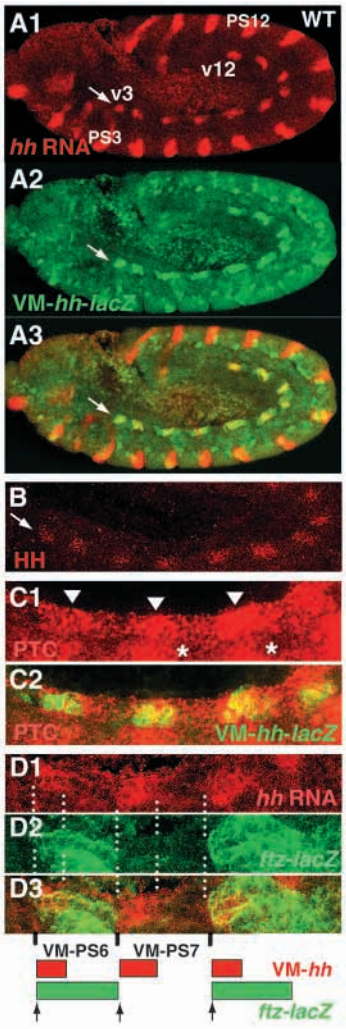

Fig. 1. Metameric *hh* expression in the trunk visceral mesoderm. *hh* expressions in wild-type embryos at late stage 11 (A,B,D) or mid-stage 12 (C) are shown. Lateral views of whole embryos (A,B) and enlarged VM-PSs (C,D) stained as indicated. Anterior is leftwards in this and following figures. In addition, except for Figs 4, 6, 7, white arrows indicate VM. PSN and vN (N, numeral), respectively, indicate ectodermal parasegment number and VM-PS number. (A) *hh* RNA (A1, red) and VM-*hh-lacZ* (A2, green) expression. (A3) Merged picture. (B) HH protein expression. (C) PTC (C1,2, red) and VM-*hh-lacZ* (C2, green) expression. Arrowheads, PTC signals in VM. Asterisks, ectodermal PTC signals. (D) *hh* RNA (D1, red) and *ftz-lacZ* (D2, green). (D3) Merged picture. *hh* RNA and *ftz-lacZ* expression indicate that VM-*hh* expression occurs in the anterior terminal region of each VM-PS. Interpretation of D1-3 is shown at the bottom.

TIN and *bap-lacZ* or *bnl* RNA (Fig. 2F,G) indicated that *tin*, *bap* and *bnl* were co-expressed in VM-PS3-12 during stage 11; in VM-PS2, only *bnl* was expressed. Stage 11-12 VM was also stained for TIN and VM-*hh-lacZ* (Fig. 2H). TIN and VM-*hh-lacZ* expression partially overlapped. VM-*hh* expression in the anterior terminal region of VM-PSs (see Fig. 1D) indicated that each *tin*/*bnl*/*bap* trio expression domain straddles the VM-PS boundary (see Fig. 2I).

In summary, VM-PSs in thorax and abdomen, respectively, was found to be subdivided into five or six regions with respect to differential expression of VM-metameric genes at stages 11-12 (Fig. 2I).

Requirements of *hh* and *wg* signals for VM-PS gene expression

VM-PS cell fates may be governed by ectodermal HH and WG signals (Bilder and Scott, 1998). Thus, we examined the effects of changing *hh* or *wg* activity on VM-PS gene expression at late stage 11 to early stage 12. For misexpression of *hh* or *wg*, 24B-GAL4 or *twi*-GAL4 were used as mesodermal-GAL4 drivers (Brand and Perrimon, 1993; Greig and Akam, 1993).

As shown in Fig. 3A-C, VM-*hh* expression was abolished in both hh^{13C} and wg^{CX4} embryos, while VM-*hh* expression was expanded throughout VM in response to misexpression of *wg* (Fig. 3D) and some expansion was noted due to *hh* misexpression (Fig. 3N,O). As *hh* and *wg* expression is mutually regulated in early embryogenesis (Ingham, 1993), the above finding may indicate that either *hh* or *wg*, or both, is required for VM-*hh* expression. Should WG be a primary effector but HH not, VM-*hh-lacZ* misexpression may be expected to occur in *hh* mutants that misexpress *wg*. To provide clarification of this point, *hh* and *wg* were misexpressed on *wg* and *hh* mutant backgrounds, respectively. No positive VM-*hh* signals could be found in either case (Fig. 3E,F). Previous studies suggested that *hh* mutants with ectopic *wg* fail to form VM due to earlier patterning functions of these genes (Azpiazu et al., 1996). However, we found that VM, incompletely expressing TIN, is formed under our experimental conditions (Fig. 3G). It may thus follow that the concerted action of WG and HH, both of which serve as primary positive regulators, is required for VM-*hh* expression.

The effects of change in *hh* and *wg* activity on *tin*, *bnl* and *bap* expression in VM were very similar, if not identical, to each other. The expression of *tin*, *bnl* and *bap* at late stage 11 was significantly reduced or hardly present in the absence of *wg* activity (Fig. 3H,I). The expression of these VM metameric genes expanded into nearly all VM cells on misexpression of *wg* (Fig. 3J), indicating that WG serves as a positive regulator of *tin*/*bnl*/*bap* expression in VM. HH may have little or no role in *tin*/*bnl*/*bap* expression in stage 11 VM. Neither appreciable expansion nor reduction in *tin*/*bnl*/*bap* domains could be observed with mesodermal *hh* misexpression (compare Fig. 3M with 3L). In hh^{13C} embryos, *tin*/*bnl*/*bap* expression appeared to have expanded in VM (Fig. 3K). But in hh^{13C} embryos, the number of FAS3-positive VM-PS cells was reduced by about a half (see below) and the number of *tin*/*bnl*/*bap*-positive cells per VM-PS was virtually the same as that in wild type (data not shown). The absence of *tin*/*bnl*/*bap*-negative cells in hh^{13C} embryos may thus be a reflection of partial failure of VM cell formation in *hh* mutants.

It is evident from the above that *wg* is required for *tin*/*bnl*/*bap* trio expression. Why was TIN was detected in hh^{13C} embryos, which possibly lack *wg* expression owing to mutual regulation between *wg* and *hh*? In hh^{13C} embryos, only dorsalmost WG, which is required for *tin*/*bnl*/*bap* expression, was still found to be expressed in hh^{13C} embryos at stages 10-11, even with virtual elimination of other *wg* signals (data not shown).

The fact that *hh* misexpression does not change *tin* expression in VM allowed us to examine whether VM-*hh* expression occurred anteriorly or posteriorly subsequent to *hh*

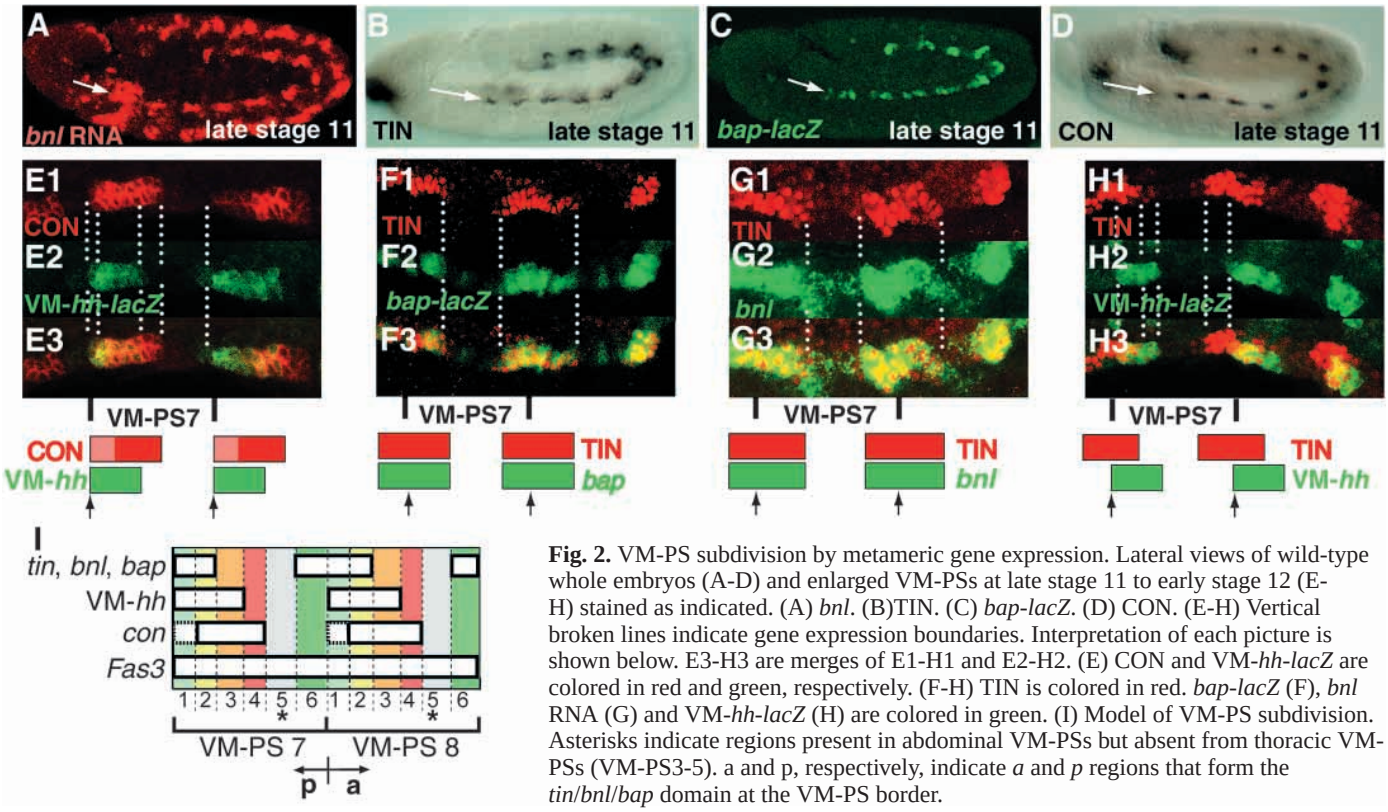

Fig. 2. VM-PS subdivision by metameric gene expression. Lateral views of wild-type whole embryos (A-D) and enlarged VM-PSs at late stage 11 to early stage 12 (E-H) stained as indicated. (A) *bnl*. (B)TIN. (C) *bap-lacZ*. (D) CON. (E-H) Vertical broken lines indicate gene expression boundaries. Interpretation of each picture is shown below. E3-H3 are merges of E1-H1 and E2-H2. (E) CON and VM-*hh-lacZ* are colored in red and green, respectively. (F-H) TIN is colored in red. *bap-lacZ* (F), *bnl* RNA (G) and VM-*hh-lacZ* (H) are colored in green. (I) Model of VM-PS subdivision. Asterisks indicate regions present in abdominal VM-PSs but absent from thoracic VM-PSs (VM-PS3-5). a and p, respectively, indicate *a* and *p* regions that form the *tin*/*bnl*/*bap* domain at the VM-PS border.

misexpression. VM cells misexpressing *hh* were stained for TIN and VM-*hh-lacZ*. As shown in Fig. 3N,O, *hh* misexpression brought about the anterior expansion of VM-*hh*.

Crucial periods of ectodermal HH and WG action for VM metameric gene expression

To determine when ectodermal HH and WG required for VM-metameric gene expression is produced, *hh* and *wg* activity was transiently altered using temperature sensitive *hh* ($hh^{9K/13C}$; hh^{ts}) and *wg* (wg^{IL4}; wg^{ts}) mutants. *hh* activity was eliminated by shifting-up hh^{ts} embryos from permissive (18°C) to non-permissive (29°C) temperatures at stage 10 to early stage 11. As shown previously for *con* expression (Bilder and Scott, 1998), metameric VM-*hh* (VM-*hh-lacZ*) expression, which normally becomes discernable at mid- to late stage 11, disappeared (Fig. 4A,B). By contrast, *con* and VM-*hh* expression was normal after temperature shift-up at mid stage 11 or later (Fig. 4A,C). With temperature shifted down from non-permissive to permissive temperatures at the end of stage 9 to early stage 10, expression patterns of VM-*hh* and all other VM genes examined here were very similar or even identical to those in wild type (Fig. 4A,D), although progenitor cell number per VM-PS unit (VM-PS cell number) was reduced to 60-70% that of wild type (data not shown). HH produced during stage 10 to early stage 11 should thus be considered essential for initiation of VM-*hh* as well as *con* expression. HH secreted before the end of stage 9 or after mid-stage 11 onwards should be dispensable at least for initiation of VM-*hh* expression. Similar results have been reported in the case of *con* expression by Bilder and Scott (Bilder and Scott, 1998). In contrast to VM-*hh* and *con* expression, the expression of *tin* and of *bnl* and *bap* (Fig. 4A,E and data not shown) was normal with or without *hh* activity; this again demonstrated that *hh* is not involved in *bnl*, *tin* or *bap* expression.

As in the case of HH, the shift-up study indicated that WG produced during stage 10 was required for *hh* and *tin* expression in VM (Fig. 4F,G,N) but not expression of *con* (Fig. 4F,H). Nevertheless, WG produced at early stage 11 is essential for *tin* expression but dispensable for that of VM-*hh* (Fig. 4F,I). WG produced at mid stage 11 or later was apparently unnecessary for either (Fig. 4F). Shift-down experiments indicated that WG produced at and before the end of stage 9 to early stage 10 is dispensable for VM-*hh* and *tin* expression (Fig. 4F,J) and it follows that WG produced during stage 10 to early stage 11 regulates the expression of *hh* and *tin* expression.

hh and *wg*, expressed in ectoderm from stage 5 onwards (Tabata et al., 1992; Baylies et al., 1995), is not detectable in mesoderm by stages 9-10 (data not shown). Mesodermal *hh* was again seen at mid-stage 11 (see Fig. 1A1,B), while that of *wg* is reported to start at mid-stage 11 only in VM-PS8 (Immergluck et al., 1990). Our results would thus mean that HH and WG emanating from the ectoderm during stage 10 to early stage 11 regulate the expression of VM-metameric genes.

Each *tin*/*bnl*/*bap* domain consists of a posterior terminal region of one VM-PS and anterior terminal region of its posterior neighbor (*p* and *a* regions, respectively; Fig. 2I, Fig. 4K). The latter is always close to the ectodermal AP border during early stage 10 to mid-stage 11, while the former is so only at late stage 10 to mid-stage 11 (Borkowski et al., 1995) (see also Fig. 8). Consistent with this, examination of wg^{ts} embryos shifted-up at late stage 10 to early stage 11 indicated that an appreciable fraction of embryos possess VM with TIN and *bnl* signals only in the *a* region of VM-PSs (Fig. 4L,M). While no *tin* expression occurred in embryos shifted-up from

early stage 10 onwards (Fig. 4N), TIN signals were detected only in a few *p*-region cells near the VM-PS border in a fraction of embryos shifted-up at late stage 10 to early stage 11 and shifted-down at mid-stage 11 (see Fig. 7F1). In addition, in contrast to an earlier report (Azpiazu and Frasch, 1993), we found that, in wild-type VM, *tin* RNA signals change much more dynamically than do *tin* protein signals at late stage 10 to early stage 11 (compare Fig. 4O1 with 4O2,3). In slightly younger embryos, *tin* RNA signals were detected only in the *a* region of each VM-PS (Fig. 4O2), while, in older ones, *tin* RNA signals were detected in both *a* and *p* regions (Fig. 4O3). No corresponding protein signal change could be detected possibly because TIN is much more stable than *tin* RNA (Fig. 4O1 and data not shown). The *tin*/*bnl*/*bap* expression within each VM-PS is thus reasonably concluded under the control of WG signals emanating from two distinct sources at different times (see Fig. 8).

Effects of *hh* and *wg* activity change on VM cell formation

FAS3 is expressed throughout VM from mid stage 11 onwards (Fig. 3P). Thus, using anti-FAS3 antibody staining, VM-PS cell number in mid stage 11 embryos differing in HH and WG signaling activity was examined. In hh^{13C} and wg^{CX4} embryos, this cell number was reduced to about a half and two thirds that of wild type (17 cells), respectively (Fig. 3P-R), but was not affected by mesodermal overexpression of *hh* or *wg* or transient loss of *hh* and *wg* activity at stage 10 (Fig. 3S and data not shown). Variation in *hh* or *wg* activity at stage 10 thus has no significant effect on VM-PS cell formation.

VM-*hh* is required for maintenance of its own expression

At mid-stage 11 and later, VM cells are situated far away from ectoderm and, consequently, HH signals possibly required for VM development from mid-stage 11 onwards may not come from *hh* ectodermal domains. The activity of VM-*hh*, whose expression starts at mid stage 11, was eliminated by shifting-up hh^{ts} embryos from permissive to non-permissive temperatures. A 90-minute elimination of *hh* activity during mid-stage 11 to mid-stage 12 resulted in loss of both VM-*hh* RNA and CON signals at stage 13 (Fig. 5A-D) but not those at stage 12. VM-*hh* RNA expression was also abolished by a 90-minute shifting-up from mid- to late stage 12 (data not shown). The VM expression of *ptc*, a general target gene of HH signaling, was also abolished upon elimination of *hh* activity from mid stage 11 onwards (data not shown). It may thus follow that VM-*hh*, the expression initiation of which is under the control of ectodermal HH, is essential for the maintenance of its own expression and that of *ptc*, and stage 13 *con* expression in VM.

Cubitus interruptus (Ci) is a downstream transcription factor of HH signaling and ectopic expression of the Ci repressor form in the posterior compartment of imaginal discs results in elimination of *hh* expression (Methot and Basler, 1999). Similarly, VM-*hh* was abolished by *twi*-GAL4-driven UAS-*ciNZn* encoding the Ci repressor (Hepker et al., 1997) (data not shown). 48Y-GAL4 is a GAL4 driver originally thought to be specific for endodermal expression (Martin-Bermudo et al., 1997) but capable of driving target genes in VM after mid stage

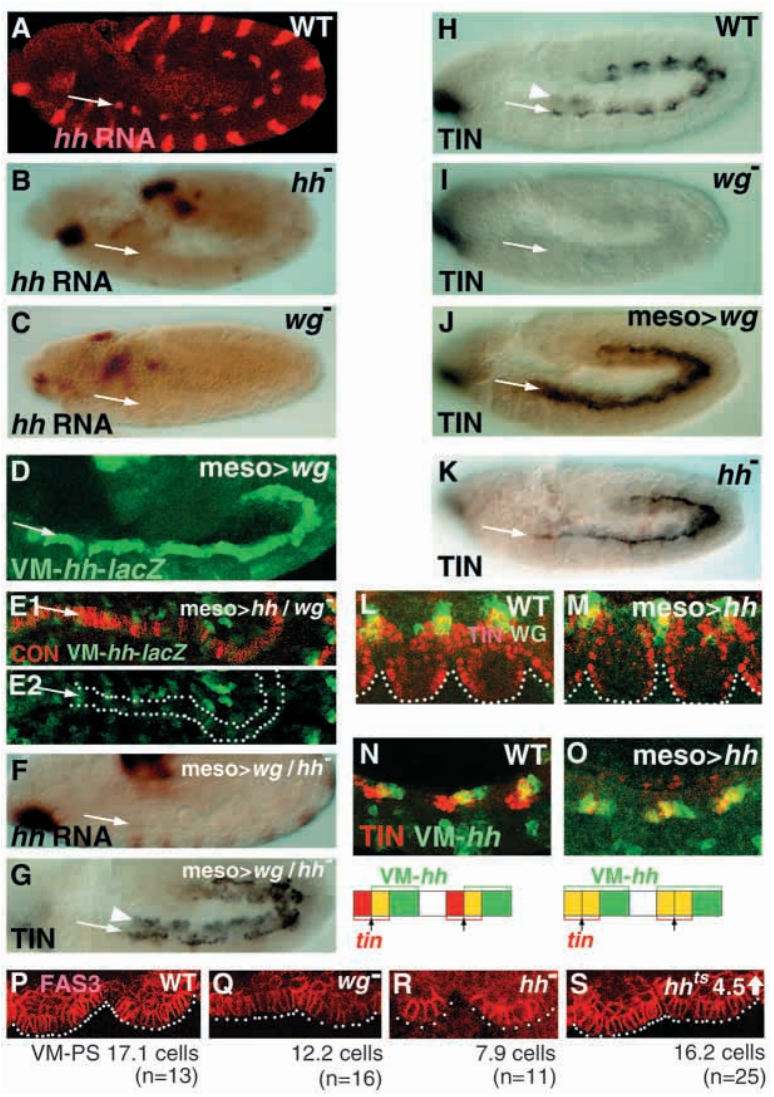

Fig. 3. Regulation of *hh* and *tin* expression and VM cell number by HH and WG. Lateral (A-K,N,O), ventrolateral (L,M) and ventral (P-S) views of early stage 11 (L,M), mid stage 11 (P-S) and late stage 11 to early stage 12 embryos (A-K,N,O) stained as indicated on various genetic backgrounds. (A,H,L,N) Wild type, (B,K) hh^{13C}, (C,I) wg^{CX4}, (D,J) UAS-*wg*/24B-GAL, (E) *twi*-GAL4/+; UAS-*hh*, wg^{CX4}/+, wg^{CX4}, (F,G) *twi*-GAL4/+; UAS-*wg*, hh^{13C}/+, hh^{13C}, (M,O) UAS-*hh*/+; 24B-GAL4/+. (B,F) Note hh^{13C} is a point mutation, which enabled us to monitor *hh* RNA expression. (F,G) Note in hh^{13C} embryo misexpressing *wg*, TIN expression in G shows VM is at least partially formed. VM is marked with CON (red; E1) or broken white lines (E2,L,M). Arrowheads in G and H indicate cardiac signals mostly out of focus. (N,O) Drawings in the lower margin show panel interpretation. (P-S) Embryos stained for FAS3. (P) Wild type, (Q) wg^{CX}, (R) hh^{13C} and (S) hh^{ts} (hh^{9K}/hh^{13C}) embryos shifted-up from early stage 10 (4.5 AEL) onwards. Broken white lines indicate VM progenitors. Average cell numbers per VM-PS are shown below. meso in E-G,M,O indicates that the expression of target genes is driven by GAL4 drivers. Arrows in A-K indicate VM.

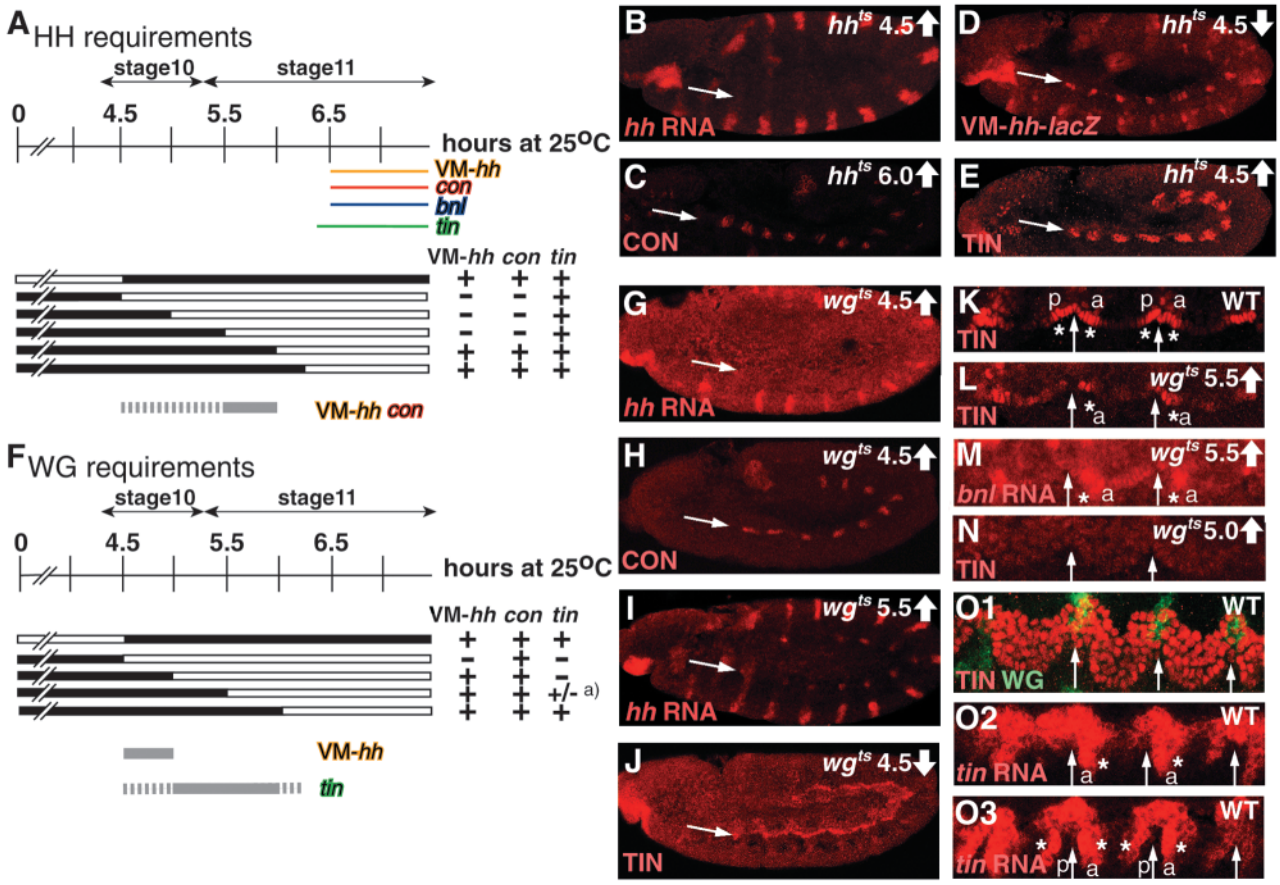

Fig. 4. Determination of the critical period sensitive to HH and WG signals, using hh^{ts} (hh^{9K}/hh^{13C}) and wg^{ts} (wg^{IL114}) mutants. (A,F) Black boxes, permissive temperature (18°C); white boxes, non-permissive temperature (29°C). Developmental time in this and subsequent sections is shown by time after egg laying (AEL) at 25°C. *tin*, *con* and VM-*hh* expression was examined at late stage 11 to early stage 12. +, normal or virtually normal expression; –, no expression; a), abnormal restriction of expression area (see L-N). Horizontal lines show metameric expression of VM-*hh* (yellow), *con* (red), VM-*bnl* (blue) and *tin* (green) in wild type. Gray bars associated with thick gray broken lines, deduced critical periods when VM-*hh*, *con* and *tin* are sensitive to HH (A) or WG (F). (B-E,G-N) Examples of shift-up/down effects on expression of three VM-metameric genes. hh^{ts} (B-E) and wg^{ts} (G-N) embryos were shifted down (D,J) or up (B,C,E,G-I,L-N) at indicated time AEL. (B-E,G-J) Lateral views of late stage 11 to early stage 12 embryos stained as indicated. (K-N) Ventral views of mid-stage 11 VM. Asterisks indicate expression of TIN (K,L) and *bnl* (M). (K) Wild type. a and p indicate *a* and *p* regions of VM-PSs, respectively. (L,M) Elimination of *wg* activity from early stage 11 on caused TIN/*bnl* expression only in posterior halves of the presumptive expression domains, which correspond to the anterior terminal region of each VM-PS. (N) Elimination of TIN activity from mid-stage 10 in response to absence of *wg* activity from mid-stage 10. (O) Ventrolateral views of wild-type early stage 11 VM. O2 is slightly younger than O3. Asterisks indicate *tin* RNA expression. Arrows in B-E,G-J indicate VM; arrows in K-O3 indicate VM-PS boundaries.

11 (data not shown). When UAS-*ciNZn* was driven by 48Y-GAL4, maintenance but not initiation of VM-*hh* expression was impaired (Fig. 5E,F). Thus, both initiation and maintenance of VM-*hh* appear to be negatively regulated by Ci repressor misexpression.

Requirements of VM-*hh* for normal gastric caecum formation

As with *dpp* and *wg* expressed in VM-PS7 and 8, respectively (Szuts et al., 1998), VM-*hh* may be required for endodermal cell differentiation. To clarify this point, VM-*hh* activity was abolished and possible morphological changes of VM derivatives were observed at 25 hours AEL. hh^{ts} embryos were shifted up from permissive to non-permissive temperatures for 3 hours during mid-stage 11 to late stage 12. The majority of embryos were associated with the short gastric caecum phenotype (Fig. 6A,D), while, in about 10% of the total (n=57), one or a few gastric caeca were lost and the size of those remaining was considerably reduced (Fig. 6F). A similar short gastric caecum phenotype was also observed in virtually all embryos with UAS-*ciNZn* driven by 48Y-GAL4 (Fig. 6G). As described above, in these embryos, VM-*hh* RNA expression is normally initiated but not maintained, while ectodermal *hh* expression appears normal, indicating that they possess normal ectodermal HH activity but lack VM-HH activity during most of late developmental stages. VM-*hh* thus appears essential for normal gastric caecum formation.

Gastric caeca are derivatives of precursors consisting of VM-PS3 cells and immediately adjacent endodermal cells (Reuter and Scott, 1990; Bate, 1993; Szuts et al., 1998) and all four gastric caecum invaginations become apparent by stage 17 (16 hours AEL) (Reuter and Scott, 1990). While a considerable

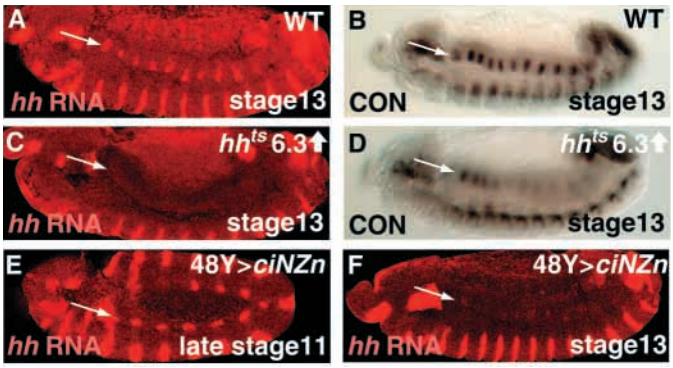

Fig. 5. Involvement of VM-*hh* in VM-PS subdivision. (A,B) Wild type. (C-D) *hh*^{ts}. (E,F) 48Y-GAL4/UAS-*ciNZ*n. Late stage 11 (E) and stage 13 (A-D,F) embryos stained as indicated. (A-D) Elimination of *hh* activity during mid stage 11 to stage 12 (6.3~7.8 AEL) did not perturb the initiation of CON and VM-*hh* (data not shown), but caused loss of their expression at stage 13 (C,D). Note that CON expression in VM-PS3-5 still persists, even in the complete absence of *hh* activity (D; data not shown). (E,F) VM-*hh* expression was virtually normally initiated (E), but could not persist when UAS-*ciNZn* was driven by 48Y-GAL4 (F).

fraction of gastric caecum precursors express *DWnt-4* (Graba et al., 1995), anterior VM-PS3 cells are positive for VM-*hh* (Fig. 6C). Because, in VM, PTC signal, which serves as a marker for the area with high levels of HH reception, was restricted to cells expressing VM-*hh* and their vicinity (see Fig. 1C), we believe that VM-PS3 must provide HH required for normal gastric caecum formation.

It should, however, be noted that the above conclusion does not necessarily exclude the possibility that ectodermal *hh* may have some essential roles in gastric caecum formation at earlier stages. Indeed, gastric caecum phenotypes more severe than those described above were found in *hh*^{ts} embryos shifted-up during stage 10-11, and in those with UAS-*ciNZn* driven by 24B-GAL4 or *bap*-GAL4 (Zaffran et al., 2001) (Fig. 6I and data not shown). Gastric caecum was virtually completely abolished in *hh*^{13C} and *twi*-GAL4-driven UAS-*ciNZn* embryos (Fig. 6J,L). We interpret these findings as suggesting that there are multiple steps requiring *hh* activity for normal gastric caecum formation.

Short gastric caecum phenotypes have also been reported in *dpp* hypomorphic mutants and *vein* (*vn*) mutants (Bate, 1993; Szuts et al., 1998). *dpp* is expressed in VM-PS3 from stage 11 onwards and its expression area virtually overlaps that of VM-*hh-lacZ* expression (Bate, 1993) (Fig. 6B), while VM-*vn*, whose expression is maintained by VM-PS3 *dpp* (Szuts et al., 1998), is restricted to VM-PS2-4 from stage 13 onwards (Szuts et al., 1998). The complete absence of *dpp* activity from VM-PS3 has been reported to induce the gastric caecum-less phenotype (Hursh et al., 1993; Masucci and Hoffmann, 1993). Thus, examination was made of whether *dpp* expression is reduced or abolished in *hh*^{ts} embryos shifted up during mid-stage 11 to late stage 12 and 48Y-Gal4-driven UAS-*ciNZn* embryos, along with *hh*^{13C} and *twi*-GAL4-driven UAS-*ciNZn* embryos. *dpp* expression was observed at stage 13. As shown

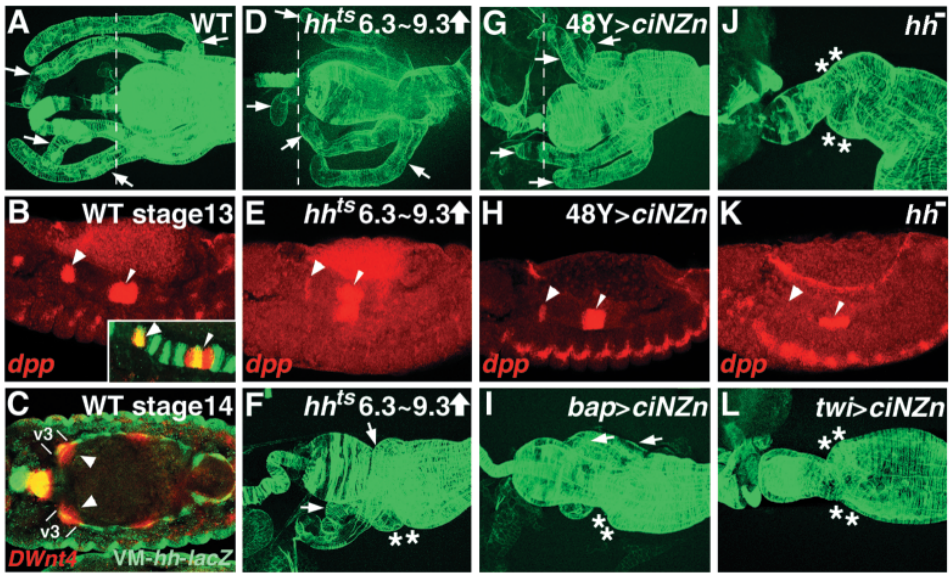

Fig. 6. *hh* regulates gastric caecum development through *dpp* expression regulation. (A,D,F,G,I,J,L) Guts dissected at 25 AEL stained with phalloidin-FITC. Arrows indicate gastric caecum evaginations; asterisks indicate eliminated gastric caeca. Compare the gastric caecum size using the vertical broken line as a measure. (B,E,H,K) *dpp* RNA expression in stage 13 embryos with HH signaling defects. Large arrowheads indicate *dpp* expression in VM-PS3. *dpp* expression in VM-PS6,7 serves as an internal control (small arrowheads). (A-C) The wild-type embryo possesses four long evaginations of gastric caecum with similar size. In wild type, VM-PS3 *dpp* (red) expression almost overlapped that of VM-*hh-lacZ* (green) (inset in B). (C) The dorsal view of a wild-type stage 14 embryo stained for *Dwnt4* RNA (red) and VM-*hh-lacZ* (green). Arrowheads indicate VM-PS3 gastric caecum primordia with *hh* expression. In *hh*^{ts} embryos shifted-up during mid-stage 11 to late stage 12 (6.3-9.3 AEL), gastric caeca were shortened or eliminated (D,F) and VM-PS3 *dpp* expression was significantly reduced in area and intensity (E). In embryos with 48Y-GAL4-driven UAS-*ciNZ*n, gastric caecum was always short (G) and VM-PS3 *dpp* expression was reduced (H). (I) *bap*-GAL4/+; UAS-*ciNZ*n/+ embryo. In *hh*^{13C} (J) or *twi*-GAL4/+:UAS-*ciNZ*n embryos (L), gastric caecum evagination was barely detectable. In these embryos, *dpp* expression in VM-PS3 was abolished (K; data not shown).

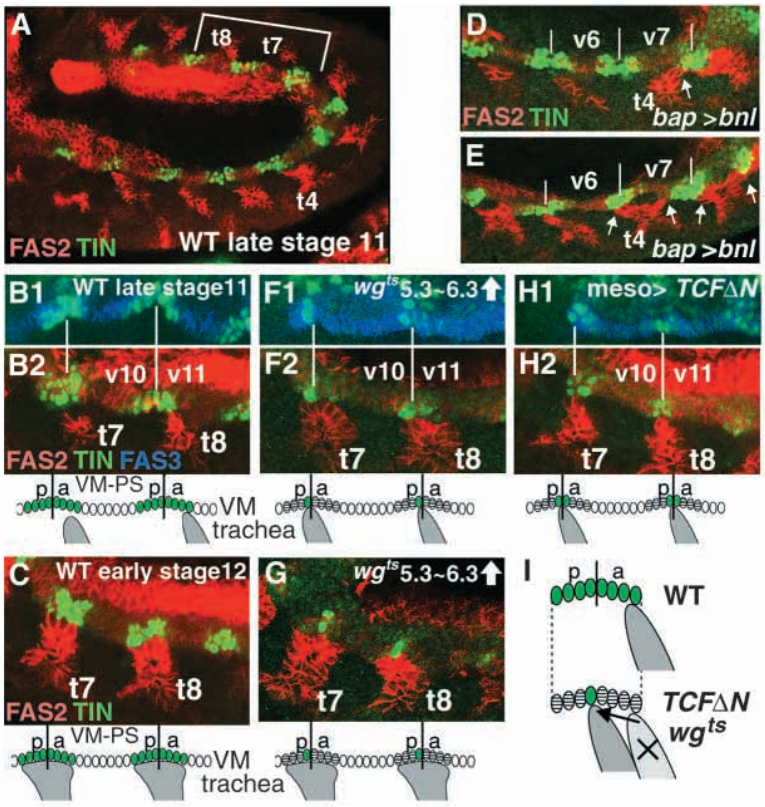

Fig. 7. Roles of VM-*bnl* in tracheal development. vN and tN (N is an arbitrary integer) indicate VM-PS and Tr number, respectively. (A-C) Wild type. (D,E) *bap*-GAL4/+; UAS-*bnl*/+. (F,G) wg^{ts} embryo shifted up during early mid-stage 11 (5.3~6.3AEL). (H) *twi*-GAL4/+; UAS-*dTCF*-ΔN/+. Late stage 11 to early stage 12 embryos are stained with FAS2, TIN or FAS3 as indicated. Lateral views are shown except for (B1, F1, H1), which are ventral views. Vertical bars, VM-PS borders. Panel interpretation is shown below. The region labeled with a bracket in A is enlarged in B2. (A-C) Relationship between VB budding and VM-*bnl* expression in wild type. (A) VB buds towards VM-*bnl* domains in a 1:1 fashion at late stage 11. (B) VB of Tr8 first touches the posterior vicinity of the TIN-expressing *a* region of VM-PS11. (C) At early stage 12, several cells touch with the *p* and *a* region expressing *tin*/*bnl*. (D,E) Misexpression of *bnl* in the entire VM caused misrouting (D) or bifurcation (E) of VB (arrows). (F-H) Reduction of *tin*/*bnl* expression domain using wg^{ts} mutant (F,G) or UAS-*dTCF*-ΔN (H) causes misrouting of VB towards the *p* region of VM-PS10 (F2) or VM-PS10-11 border (H2), respectively. (I) VB shift in *wg* or WG signaling mutants is schematically shown.

in Fig. 6B,E,H,K, the *dpp* RNA expression levels in these HH signaling mutants were roughly proportional to the gastric caecum length. That is, in the hh^{ts} embryos shifted up during mid-stage 11 to late stage 12 and 48Y-Gal4-driven UAS-*ciNZn* embryos, both exhibiting the short gastric caecum phenotype (see Fig. 6D,G), VM-PS3 *dpp* expression was significantly reduced (Fig. 6E,H), whereas, in hh^{13C} embryos and *twi*-GAL4-driven UAS-*ciNZn* embryos, both of which completely lack the gastric caecum (see Fig. 6J,L), no *dpp* signals were detected in VM-PS3 (Fig. 6K and data not shown). Moreover, *vn* expression in VM-PS2-4 was significantly reduced or virtually completely abolished in these HH signaling mutants (data not shown). It may thus follow that the concerted action of HH secreted at stages prior to stage 11 and HH from VM-PS3 at later stages establishes the normal expression level of *dpp* in VM-PS3, and most, if not all, gastric caecum defects of these HH signaling mutants are attributed to reduction or loss of *dpp* expression in VM-PS3.

Regulation of tracheal visceral branch migration through VM metameric BNL

Tracheal cells are formed from 10 clusters (Tr1-10) of ectodermal cells on each side of the embryo. Future tracheal cell clusters invaginate, and at late stage 11, migrate to produce six primary branches, one being VB (Manning and Krasnow, 1993; Samakovlis et al., 1996). The ordered development of trachea is a consequence of communication between tracheal cells and surrounding tissues (reviewed by Zelzer and Shilo, 2000). *bnl* acts at least as a motogen for all primary branches (Sutherland et al., 1996). In parallel to and/or prior to *bnl* signaling, DPP, EGF, WG and HH are required for proper invagination of tracheal cells and guidance of specific branches (Glazer and Shilo, 2001). Integrin proteins have been recently shown involved in VB guidance after VB reaches VM (Boube et al., 2001). Mesodermal cells may also be required for assisting or constraining tracheal branching (Franch-Marro and Casanova, 2000; Wolf and Schuh, 2000). No branch formation occurs in *bnl* mutants and ectopic *bnl* expression redirects some branches (Sutherland et al., 1996), but whether restricted *bnl* expression in VM is essential for VB guidance remains unclear.

VB cells, though not those in Tr3 or Tr9 (Manning and Krasnow, 1993; Sutherland et al., 1996), begin budding towards corresponding *bnl* expression domains in a 1:1 fashion at late stage 11 (Fig. 7A). The tip of VB of Tr-(*i*-3) (*i*; integer) first appeared to touch the vicinity of the posterior end of the *a* region or *bnl*/TIN-expressing anterior region of VM-PS-*i* (Fig. 7B) and then, VB/VM contact expanded to the entire VM-PS-(*i*-1) *p*-region and VM-PS-(*i*) *a*-region (Fig. 7C). During stage 12, with *bnl* expression becoming rather homogeneous throughout VM (data not shown), VB extends further anteriorly. This extension depends on integrin genes (Boube et al., 2001).

The expression of *bnl* was changed to examine how this would affect initial VB budding at stage 11 to early stage 12, which is independent of integrin genes (Boube et al., 2001). First, *bnl* was misexpressed in the entire VM with *bap*-GAL4. Should VM-BNL serve as a chemoattractant for VB guidance, considerable VB misrouting would be expected to occur upon *bnl* misexpression. We found 48 VB bifurcations (23%) and five simple VB misroutings (2.4%) in 210 VM-PSs normally capable of coming into contact with VB (Fig. 7D,E). These defects appear to be persisted at least until stage 15. Fig. 7D,E also shows that no appreciable change in *tin* expression was induced by *bnl* misexpression in VM. Thus, VB misrouting and bifurcation appear solely due to *bnl* misexpressed in VM.

The *bnl*/*tin* expression domain in VM-PSs was reduced in

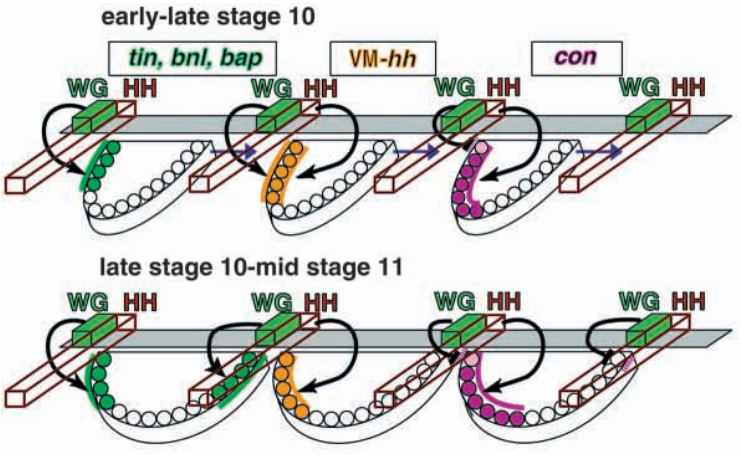

Fig. 8. Model of transcriptional regulation of VM-metameric genes during stages 10-11. Ventrolateral view of VM is shown schematically. Gray strip, ectodermal cell layer. Green and brown-outlined boxes, ectodermal WG and HH sources, respectively. Blue horizontal arrows in the top diagram show the posterior expansion of the VM competent region; black arrows indicate activation; black-T-shaped-lines indicate repression. WG and HH susceptible regions are shown by colored lines along the future VM. *tin*/*bnl*/*bap* (green), VM-*hh* (yellow) and *con* (crimson) expression are indicated. Reduced *con* expression at the anterior end of VM-PSs is indicated in pink. For simplicity, three gene groups are separately depicted in three successive VM-PSs. See the text for details.

area in two ways, both dependent on WG being a positive regulator of metameric expression of *bnl* and *tin* in VM. As TIN and *bnl* are co-expressed in both wild-type and *wg* hypomorphic mutant conditions, TIN was used as an area marker for *bnl* expression. *dTCF-ΔN* is a dominant negative form of *d-TCF* and serves as an antagonist of WG signaling (Cavallo et al., 1998). *twi*-GAL4-driven UAS-*dTCF-ΔN*, which blocks WG signaling in a mesoderm-specific manner, restricted TIN/*bnl* expression only to cells in the vicinity of the VM-PS border (Fig. 7H,I). In these mutant flies, the remnant TIN/*bnl*-expressing *p/a*-border-cells served as targets for the initial VB contact (Fig. 7H); unlike the situation in wild type, no initial VB/VM contact was detected at the vicinity of the putative posterior end of the VM-PS *a* region (Fig. 7I).

A similar redirection of VB migration was also observed in wg^{ts} mutants shifted-up for 60 minutes from late stage 10 to stage 11. In this case, the remnant TIN/*bnl*-expressing *p*-region cells near the VM-PS border served as targets for the initial VB contact (Fig. 7F). Subsequently, VM/VB contact expanded, as in wild type (Fig. 7G). Based on these results, we conclude that metameric BNL within VM serves as a chemoattractant for initial VB migration.

DISCUSSION

Subdivision of VM parasegment into five or six domains

Previous analysis of *con* expression by Bilder and Scott (Bilder and Scott, 1998) indicated that VM-PSs are subdivided by the concerted action of *hh* and *wg* into at least two domains. We now extended this finding through use of a greater number of trunk visceral mesodermal genes, including *hh* and *bnl*. Detailed analysis of VM-*hh*, *bnl*, *tin* and *bap* expression in addition to *con* indicated that trunk visceral mesodermal genes are classified into three distinct groups – *tin*/*bnl*/*bap*, VM-*hh* and *con* – and each VM-PS is subdivided into five or six regions, becoming apparent during mid stage 11 to stage 12 (see Fig. 2I).

Reiterative use of *hh* and *wg* signals in VM development

VM is presently considered to develop in two steps under the control of ectodermal HH and WG signals. First, by stage 10 (when four mesodermal primordia have become specified), VM competent or *bap* expression regions are promoted by *hh* but repressed by *wg*, via a direct targetor, *slp* (Lee and Frasch, 2000). The second surge of *hh* and *wg* activity at stages 10-11 is responsible for subdividing VM-PSs into two regions: *con* positive and negative (Bilder and Scott, 1998). Our results indicate that the expression of other four VM-metameric genes, *hh*, *tin*, *bnl* and *bap*, is also regulated by the second surge of *hh* and *wg* activity at stages 10-11.

To examine the regulation of VM-metameric genes with changing the activity of *hh* and/or *wg*, it may be necessary to evaluate the effects of possible change in cell number on VM-PS subdivision or VM-PS cell specification. In temperature-sensitive mutants of *hh* and *wg* shifted-up from stage 10, the number of VM cells positive to FAS3 at mid stage 11 on was essentially identical to that of wild type, indicating that VM-cell number change is negligible under the conditions used, while the expression of some VM metameric genes appeared compromised. In hh^{ts} mutants, VM-*hh* and *con* were not expressed, though *tin*, *bnl* and *bap* were (see Fig. 4A). In wg^{ts} mutants, VM-*hh* and *tin* were not expressed, but *con* was (see Fig. 4F). All these observations are totally in agreement with those found in simple loss-of-function and overexpression experiments, as described in the Results; under these conditions, the formation of a VM competent region should be hindered. Thus, our results may indicate that ectodermal HH and WG regulate directly, but in different ways, the expression of metameric genes in VM; VM-*hh* expression requires both HH and WG. *tin*, *bnl* and *bap* are positively regulated by WG alone, and *con* is activated by HH and repressed by WG.

Cell fate diversification within VM-PSs through concerted *hh* and *wg* signaling

In view of morphological changes in a VM competent region and consideration of our findings on VM gene regulation, the following model for VM-PS cell specification may be proposed (Fig. 8).

At stage 10 to early stage 11, anterior terminal cells of VM-PSs are presumed to be always situated near an ectodermal AP border, where they are capable of continuously receiving WG and HH signals, and WG confers competence on these cells to express *tin*/*bnl*/*bap*. WG and HH are responsible for inducing VM-*hh*, and HH, for *con* expression. In the anterior-most cells, *con* expression is reduced, which would be expected in view

of repression by high WG signal. The different thresholds of *hh* for *con* and VM-*hh* expression may explain why the *con* area expands more posteriorly compared with that of VM-*hh*. Posterior terminal VM cells, when formed, are situated far from WG expressed on the ectodermal PS border (see 'early to late stage 10' in Fig. 8). But as they migrate posteriorly and close to the posteriorly neighboring AP border by early stage 11, they become capable of receiving WG and acquire competence to express *tin*/*bnl*/*bap* (see 'late stage10 to mid-stage 11' in Fig. 8). Thus, the *tin*/*bnl*/*bap* domain would appear regulated by spatially and temporally distinct WG signals. The two-step induction of *tin/bnl/bap* expression is supported by experiments using the wg^{ts} mutant, where, either posterior or anterior expression within one patch could be differentially turned off (Fig. 4L-N). Indeed, we observed a stepwise activation of *tin/bnl* expression in VM-PSs around stage 11 (Fig. 4O). As schematically shown in Fig. 4A, *tin* and *bnl* metameric expression became apparent almost simultaneously at mid-stage 11, and our preliminary experiments showed that neither *tin* nor *bnl* misexpression could induce the ectopic expression of any other metameric genes examined here. Thus, *tin* and *bnl* expression might be initiated in a mutually independent manner.

This VM-PS subdivision model should be modified when applied to thoracic segments, where *hh* may not be the sole determinant of *con* expression (Zaffran et al., 2001) (see Figs 2, 5; data not shown).

Requirements of VM-*hh* for segmental subdivision of VM-PSs and gastric caecum formation

Our study strongly suggested that metameric VM-*hh* is required for the maintenance of its own as well as metameric *con* expression (see Fig. 5C,D), although the latter becomes independent of VM-*hh* at late stages (C. H., unpublished). That PTC, a direct target of *hh*, is upregulated in each VM-*hh* expression domain at stage 12, at that time VM is far away from the epidermis or ectodermal HH sources (see Fig. 1C), is another evidence supporting the notion that *hh* signaling caused by metameric VM-*hh* is operative in VM.

Our results (Fig. 6) also showed that HH is required for gastric caecum development. HH may operate in multiple steps in mesoderm and its source for the last step is VM-HH emanating from VM-PS3, a part of the future gastric caecum region. Fig. 6 also indicated that most, if not all, gastric caecum defects found in HH signaling mutants may be due to the reduction or loss of VM-PS3 *dpp*, whose production is under the control of VM-PS3 HH and HH at stages prior to stage 11 (this work) (Hursh et al., 1993; Masucci and Hoffmann, 1993). *vn* expression, which is positively controlled by VM-PS3 *dpp* (Szuts et al., 1998), was also significantly reduced in HH signaling mutants (data not shown), while *Dwnt4* expression was not seriously affected even in *hh* null mutants (C. H., unpublished). Thus, the effect of *hh* activity loss on gastric caecum formation may be due to partial changes in fate/transcription programs of VM-PS3 cell precursors.

VM BNL may serve as a chemoattractant for VB migration

Reiterative *bnl* expression in VM is likely to be a determinant of the particular mode of VB migration. The tip of VB first came in touch with the vicinity of the posterior end of the *tin*/*bnl*/*bap* expressing *a* region, where all the five metameric genes examined are expressed (Fig. 7A,B). BNL misexpression with VM-specific-GAL4 drivers induced VB misrouting and bifurcation (Fig. 7D,E) but neither *hh* misexpression nor transient loss of HH activity during stage 11 had any effect on VB budding (C. H., unpublished). BNL misexpression brought about no significant change in expression of *tin* (Fig. 7D,E), while restriction of the *tin*/*bnl*/*bap* expression domain using either *dTCF*-ΔN or wg^{ts} caused a shift in the first VB/VM contact point (Fig. 7I). Furthermore, under a *wg* mutant condition, no change could be detected in VM-*hh* or in *con* expression (see Fig. 4F). Thus, only the *bnl* expression appears to be closely correlated with VB budding, strongly suggesting that BNL serves as a chemoattractant for initial VB migration.

We thank Drs R. White, M. Frasch, C. S. Goodman, M. Krasnow, T. Tabata, I. Guerrero, J. Pradel, T. Orenic, T. Volk, the DSHB, and the Bloomington Stock Center for antibodies, cDNA and fly strains. We thank all colleagues in the laboratory, especially T. Kojima. This study was supported in part by grants from the Ministry of Education, Culture, Sport, Science and Technology of Japan to K. S.

REFERENCES

Alcedo, J. and Noll, M. (1997). Hedgehog and its Patched-Smoothened receptor complex: a novel signaling mechanism at the cell surface. *Biol. Chem.* **378**, 583-590.

Azpiazu, N. and Frasch, M. (1993). tinman and bagpipe: Two homeobox genes that determine cell fates in the dorsal mesoderm of *Drosophila*. *Genes Dev.* **7**, 1325-1340.

Azpiazu, N., Lawrence, P. A., Vincent, J. P. and Frasch, M. (1996). Segmentation and specification of the Drosophila mesoderm. *Genes Dev.* **10**, 3183-3194.

Baylies, M. K., Arias, M. and Bate, M. (1995). *wingless* is required for the formation of a subset of muscle founder cells during *Drosophila* embryogenesis. *Development* **121**, 3829-3837.

Baylies, M. K., Bate, M. and Gomez, M. R. (1998). Myogenesis: a view from *Drosophila*. *Cell* **93**, 921-927.

Bate, M. (1993). The mesoderm and its derivative. In *The Development of* Drosophila melanogaster (ed. M. Bate and A. Martinez-Arias), pp 1013-1090. Plainview, NY: Cold Spring Harbor Laboratory Press.

Bienz, M. (1994). Homeotic genes and positional signaling in the *Drosophila* viscera. *Trends Genet.* **10**, 22-26.

Bienz, M. (1997). Endoderm induction in *Drosophila*: The nuclear targets of the inducing signals. *Curr. Opin. Genet. Dev.* **7**, 683-688.

Bilder, D. and Scott, M. P. (1998). *Hedgehog* and *wingless* induce metameric pattern in the *Drosophila* visceral mesoderm. *Dev. Biol.* **201**, 43-56.

Bodmer, R. (1993). The gene *tinman* is required for specification of the heart and visceral muscles in *Drosophila*. *Development* **118**, 719-729.

Borkowski, M., Brown, N. H. and Bate, M. (1995). Anterior-posterior subdivision and the diversification of the mesoderm in *Drosophila*. *Development* **121**, 4183-4193.

Boube, M., Martin-Bermudo, M. D., Brown, N. H. and Casanova, J. (2001). Specific tracheal migration is mediated by complementary expression of cell surface proteins. *Genes Dev.* **14**, 2140-2145.

Brand, A. H. and Perrimon, N. (1993). Targeted gene expression as a means of altering cell fates and generating dominant phenotypes. *Development* **118**, 401-415.

Capdevila, J., Pariente, F., Sampedro, J., Alonso, J. and Guerrero, I. (1994). Subcellular localization of the segment polarity protein patched suggests an interaction with the wingless reception complex in *Drosophila* embryos. *Development* **120**, 987-998.

Campos-Ortega, J. A. and Hartenstein, V. (1985). *The Embryonic Development of* Drosophila melanogaster. Berlin: Springer-Verlag.

Campos-Ortega, J. A. and Hartenstein, V. (1997). *The Embryonic Development of* Drosophila melanogaster. Berlin: Springer-Verlag.

Cavallo, R. A., Cox, R. T., Moline, M. M., Roose, J., Polevoy, G. A.,

Clevers, H., Peifer, M and Bejsovec, A. (1998). *Drosophila* Tcf and Groucho interact to repress Wingless signaling activity. *Nature* **395**, 604-608.

Dettman, R. W., Turner, F. and Raff, E. (1996). Genetic analysis of the *Drosophila* β3-Tubulin gene demonstrates that the microtubule cytoskeleton in the cells of the visceral mesoderm is required for morphogenesis of the midgut endoderm. *Dev. Biol.* **177**, 117-135.

Frasch, M. (1995). Induction of visceral and cardiac mesoderm by ectodermal Dpp in the early *Drosophila* embryo. *Nature* **374**, 464-467.

Franch-Marro, X. and Casanova, J. (2000). The alternative migratory pathways of the *Drosophila* Tracheal cells are associated with distinct subsets of mesodermal cells. *Dev. Biol.* **227**, 80-90.

Glazer, L and Shilo, B. Z. (2001). Hedgehog signaling patterns the tracheal branches. *Development* **128**, 1599-1606.

Graba, Y., Gieseler, K., Aragnol, D., Laurenti, P., Mariol, M., Berenger, H., Sagnier, T. and Pradel, J. (1995). *Dwnt4*, a novel *Drosophila Wnt* gene acts downstream of homeotic complex genes in the visceral mesoderm. *Development* **121**, 209-218.

Greig, S. and Akam, M. (1993). Homeotic genes autonomously specify one aspect of pattern in the *Drosophila* mesoderm. *Nature* **362**, 630-632.

Grenningloh, G., Rehm, E. J. and Goodman, C. S. (1991). Genetic analysis of growth cone guidance in *Drosophila*: Fasciclin II functions as a neuronal recognition molecule. *Cell* **67**, 45-57.

Hepker, J., Wang, Q. T., Motzny, C. K., Holmgren, R. and Orenic, T. V. (1997). *Drosophila cubitus interruptus* forms a negative feedback loop with *patched* and regulates expression of Hedgehog target genes. *Development* **124**, 549-558.

Hiromi, Y., Kuroiwa, A. and Gehring, W. J. (1985). Control elements of the *Drosophila* segmentation gene *fushi tarazu. Cell* **43**, 603-613.

Hoppler, S. and Bienz, M. (1994). Specification of a single cell type by a *Drosophila* homeotic gene. *Cell* **76**, 689-702.

Hoppler, S. and Bienz, M. (1995). Two different thresholds of wingless signaling with distinct developmental consequences in the *Drosophila* midgut. *EMBO J.* **14**, 5016-5026.

Hursh, D., A., Padgett, R., W. and Gelbart, W. M. (1993). Cross regulation of *decapentaplegic* and *Ultrabithorax* transcription in the embryonic visceral mesoderm of *Drosophila*. *Development* **117**, 1211-1222.

Immergluck, K., Lawrence, P. A. and Bienz, M. (1990). Induction across germ layers in *Drosophila* mediated by a genetic cascade. *Cell* **62**, 261-268.

Ingham, P. W. (1993). Localized *hedgehog* activity controls spatial limits of *wingless* transcription in the *Drosophila* embryo. *Nature* **366**, 560-562.

Klapper, R., Stute, C., Schomaker, O., Strasser, T., Janning, W., Renkawitz-Pohl, R. and Holz, A. (2002). The formation of syncytia within the visceral musculature of the *Drosophila* midgut is dependent on *duf*, *sns* and *mnc*. *Mech. Dev.* **110**, 85-96.

Lee, H. and Frasch M. (2000). Wingless effects mesoderm patterning and ectoderm segmentation events via induction of its downstream target *sloppy paired. Development* **127**, 5497-5508

Leptin, M. and Grunewald, B. (1990). Cell shape changes during gastrulation in *Drosophila*. *Development* **10**, 73-84.

Manning, G. and Krasnow, M. (1993). Development of the *Drosophila* tracheal system. In *The* Development of Drosophila melanogaster (ed. M. Bate and A. Martinez-Arias), pp. 609-686. Plainview, NY: Cold Spring Harbor Laboratory Press.

Martin-Bermudo, M. D., Dunin-Borkowski, O. M. and Brown, N. H. (1997). Specificity of PS integrin function during embryogenesis resides in the α subunit extracellular domain. *EMBO J.* **16**, 4184-4193.

Masucci, J., D. and Hoffmann, F., M. (1993). Identification of two regions from the *Drosophila decapentaplegic* gene required for embryonic midgut development and larval viability. *Dev. Biol.* **159**, 276-287.

Matsuzaki, M. and Saigo, K. (1996). *hedgehog* signaling independent of *engrailed* and *wingless* required for post-S1 neuroblast formation in *Drosophila* CNS. *Development* **122**, 3567-3575.

Meadows, L. A., Gell, D., Broadie, K., Gould, A. P. and White, R. (1994). The cell adhesion molecule, connectin, and the development of the *Drosophila* nueromuscular system. *J. Cell Sci.* **107**, 321-328.

Methot, N. and Basler, K. (1999). Hedgehog controls limb development by regulating the activities of distinct transcriptional activator and repressor forms of Cubitus interruptus. *Cell* **96**, 819-831.

Reuter, R. and Scott, M. P. (1990). Expression and function of the homeotic genes *Antennapedia* and *Sex combs reduced* in the embryonic midgut of *Drosophila. Development* **109**, 289-303.

Riechmann, V., Irion, U., Wilson, R., Grosskortenhaus, R. and Leptin, M. (1997). Control of cell fates and segmentation in the *Drosophila* mesoderm. *Development* **124**, 2915-2922.

Samakovlis, C., Hacohen, N., Manning, G., Sutherland, D., Guillemin, K. and Krasnow, M. (1996). Development of the *Drosophila* tracheal system occurs by a series of morphologically distinct but genetically coupled branching events. *Development* **122**, 1395-1407.

San Martin, B., Ruiz-Gomez, M., Landgraf, M. and Bate, M. (2001). A distinct set of founders and fusion-competent myoblasts make visceral muscles in the *Drosophila* embryo. *Development* **128**, 3331-3338.

Sato, M. and Saigo, K. (2000). Involvement of *pannier* and *u-shaped* in regulation of Decapentaplegic-dependent *wingless* expression in developing *Drosophila* notum. *Mech. Dev.* **93**, 127-138.

Sutherland, D., Samakovlis, C. and Krasnow, M. (1996). *branchless* encodes a *Drosophila* FGF homolog that controls tracheal cell migration and the pattern of branching. *Cell* **87**, 1091-1101.

Staehling-Hampton, K., Hoffmann, F. M., Baylies M. K., Rushton, E. and Bate, M. (1994). *dpp* induces mesodermal gene expression in *Drosophila*. *Nature* **372**, 783-786.

Suzuki, T. and Saigo, K. (2000). Transcriptional regulation of *atonal* required for *Drosophila* larval eye development by concerted action of Eyes absent, Sine oculis and Hedgehog signaling independent of Fused kinase and Cubitus interruptus. *Development* **127**, 1531-1540.

Szuts, D., Eresh, S. and Bienz, M. (1998). Functional intertwining of dpp and EGFR signaling during *Drosophila* endoderm induction**.** *Genes Dev.* **12**, 2022-2035.

Tabata, T., Eaton, S. and Kornberg, T. B. (1992). The*Drosophila hedgehog* gene is expressed specifically in posterior compartment cells and is a target of *engrailed* regulation. *Genes Dev.* **6**, 2635-2645.

Tabata, T. and Kornberg, T. B. (1994). Hedgehog is a signaling protein with a key role in pattering *Drosophila* imaginal discs. *Cell* **76**, 89-102.

Tashiro, S., Michiue, T., Higashijima, S., Zenno, S., Ishimaru, S., Takahashi, F., Orihara, M., Kojima, T. and Saigo, K. (1993). Structure and expression of *hedgehog*, a *Drosophila* segment-polarity gene required for cell-cell communication. *Gene* **124**, 183-189.

Tremml, G. and Bienz, M. (1989). Homeotic gene expression in the visceral mesoderm of *Drosophila* embryos. *EMBO J.* **8**, 2677-2685.

Weiss, J., Suyama, K. L., Lee, H. and Scott, M. P. (2001). Jelly belly: a *Drosophila* LDL receptor repeat-containing signal required for mesoderm migration and differentiation. *Cell* **107**, 387-398.

Wolf, C. and Schuh, R. (2000). Single mesodermal cells guide outgrowth of ectodermal tubular structures in *Drosophila*. *Genes Dev.* **14**, 2140-2145.

Yarnitzky, T., Min, L. and Volk, T. (1997). The *Drosophila* neuregulin homolog Vein mediates inductive interactions between myotubes and their epidermal attachment cells. *Genes Dev.* **11**, 2691-2700.

Zaffran, S., Kuchler, A., Lee, H. and Frasch, M. (2001). *biniou* (*FoxF*), a central component in a regulatory network controlling visceral mesoderm development and midgut morphogenesis in *Drosophila*. *Genes Dev.* **15**, 2900-2915.

Zelzer, E. and Shilo, B. Z. (2000). Cell fate choices in *Drosophila* tracheal morphogenesis. *BioEssays* **22**, 219-226.